



Numerical Study on Pilot Ignition of a Thermally-Thick Solid Fuel with Low-Velocity Airflow in Microgravity

Kai Zhang^{1,2} · Feng Zhu¹ · Shuangfeng Wang^{1,2}

Received: 28 September 2023 / Accepted: 12 December 2023 / Published online: 29 December 2023
© The Author(s), under exclusive licence to Springer Nature B.V. 2023

Abstract

The mechanisms controlling the dependence on low-velocity flow of the piloted ignition of a solid material under external radiant heating is investigated through a numerical modeling. The poly (methyl methacrylate) (PMMA) was used as the fuel. The objective of the present study is to gain insight into the intrinsic ignition mechanisms of a solid fuel, as well as to gain a more comprehensive understanding of the dynamical characteristics of the ignition process near the extinction limit. For this purpose, a two-dimensional numerical model has been developed using the Fire Dynamic Simulator (FDS5) code, in which both solid-phase and gas-phase reactions are calculated. Two radiant heat flux, which are 16 and 25 kW/m² were studied, and an external air flow was varied from 3 to 40 cm/s. The simulation results showed that transient gas reaction flashed before a continuous flame was attached to the sample surface for gas flow velocities lower than a critical value. As the flow velocity is reduced, the flashing time, which is defined as the time when any flame is seen above the sample surface, decreases, while the duration of flashing increases. The solid surface temperature and mass flow rate increase rapidly during flashing. The ignition time, which is defined as the time when a continuous flame is attached to the fuel surface, decreases, reaches a minimum, and then increases until ignition cannot occur. Mechanisms were considered to explain the “V-shaped” dependence of ignition time on flow-velocity, and two regimes were identified each having a different controlling mechanism: the mass transport regime where the ignition delay is controlled by the mixing of oxygen and pyrolyzate; and the heat transfer regime where the ignition delay is controlled by changes in convection heat losses and critical mass flux for ignition. With the decrease of the airflow velocity, the critical mass flux shows a trend of decreasing and then increasing, which is dominated by the mixing of the pyrolyzate and the oxidizer, while the critical temperature monotonically decreases, which is dominated by a reduction of the net heat flux at the fuel surface. The results provide further insight into the ignition behavior of solid fuel under low-velocity flow environment, and guidance about fire safety in microgravity environments.

Keywords Ignition · Solid material · Low-velocity flow · Microgravity · Critical mass flux

Introduction

Ignition is the beginning of a fire. The key parameter of flammability can be used to predict trends in flame spread rates (Fernandez-pello 1995; Lautenberger et al. 2021). Previous studies have shown that the ignition temperature, the piloted ignition delay, and the critical mass flux for ignition depend on the environmental conditions, such as the gas

flow velocity, oxygen concentration and ambient pressure (Roslon et al. 2000; Cordova et al. 2001; Zhou et al. 2003; Rich et al. 2007; McAllister et al. 2010; Fereres et al. 2015). The flow velocities induced by buoyancy are the minimum attainable during the heating and combustion process in normal gravity conditions. The ignition delay parameters are tested on this bound.

Under microgravity environment, the typical space facility environments are characterized by forced flow velocities ranging from a few millimeters to a few centimeters per second. Due to the weak convective heat transfer under microgravity conditions, the ignition of solid combustibles will be faster than that in normal gravity. However, considering the slow mass transfer rate, the ignition delay time will be increased. The two competing parallel mechanisms

✉ Feng Zhu
zhufeng@imech.ac.cn

¹ Key Laboratory of Microgravity, Institute of Mechanics, Chinese Academy of Sciences, Beijing 100190, China

² School of Engineering Science, University of Chinese Academy of Sciences, Beijing 100049, China

control solid ignition delay. Only few studies about the ignition characteristics have been performed. Fujita et al. (2000) studied the radiative ignition of a paper sheet in microgravity, and they found that the ignition delay time decreases with the increased oxygen concentration. Olson (2011) have been studied the piloted ignition of a thermally-thin solid fuel in a forced convective microgravity environment by energizing the solid fuel through a hot wire igniter, results showed that when the mixing times were very rapid, the effect of flow can be neglected for the piloted ignition, and ignition delay is dominated by the induction time, which is inversely proportional to the oxygen concentration and the total pressure.

Experimental results for thick solid ignition in microgravity were first obtained aboard KC-135 aircraft (Roslon et al. 2000). In these experiments, the ignition delay time of thick solid PMMA samples was examined in air with a low velocity in the range of 2–25 cm/s. The results showed that, in this low-velocity environment, the ignition delay time and the critical heat flux for ignition increase with the decreased flow velocity. Such an ignition behavior in a microgravity environment with low-velocity flow was also captured by numerical modeling (Zhou et al. 2003), which further predicted an easier ignition under the conditions expected in spacecraft. However, due to the insufficient microgravity time, and the severe g-jitter, which refers to small fluctuations in the g-level due to meteorological and physical events during the experiments, the buoyant flows induced by such fluctuations may exceed the very low forced flow velocity and result in increased ignition delay. Considering that the surface temperature at ignition varies at different flow velocities (McAllister et al. 2010), the ignition criterion set in numerical simulation is doubtful. Therefore, conclusions about the effect of low-velocity flow on ignition parameters should be regarded as qualitative. The ignition of a thick solid fuel has a relatively long-time scale, and the opportunity to perform space-based experiments has been scarce. In addition, conventional ignition experiments need radiative heating, which makes a high requirement on experimental resources. Therefore, it is difficult to study the microgravity ignition of a thick solid.

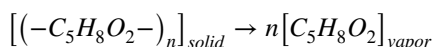
Numerical simulation provides an effective method to study the ignition behavior in a microgravity environment. Considering the ignition of solid fuels involves a complex process coupled solid and gas phases, Lautenberger et al. (2005) combined the solid phase model from Zhou et al. (2002) with the Fire Dynamics Simulator (FDS) code (McGrattan et al. 2003a, b) for the gas phase processes, and they analyzed the effect of the external radiant heat flux, the forced flow velocity and microgravity conditions on piloted ignition of a solid fuel. Following the similar approach to that of Lautenberger et al. (2005), Fereres et al. (2012, 2015) studied the influence of reduced ambient pressure and gravity

on the piloted ignition of solid materials. The present work utilizes the similar approach to that of Fereres et al. (2012, 2015) for both solid and gas phase process and emphasizes the influence of low-velocity flow on ignition in microgravity.

The focus of this study is to determine the effects of the low-velocity flow on pilot ignition of a thermally-thick solid fuel in microgravity, and to understand the controlling mechanism. The numerical simulations are performed to gather ignition data for flame behaviors during ignition, the ignition delay and the critical parameters to predict the onset of ignition for various airflows.

Numerical Modeling

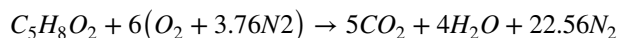
In this work, the two-dimensional numerical simulation based on Fire Dynamics Simulator (FDS5.5.3) was performed to examine the piloted ignition of a thick solid fuel. The solid-phase and gas-phase reactions were simultaneously considered in the Direct Numerical Simulation (DNS) mode. For the solid-phase reaction, the energy and mass equations were solved simultaneously, the material used in the simulation was poly (methyl methacrylate) (PMMA), and the solid-phase decomposition was performed using a one-step Arrhenius reaction with the assumption that the pyrolysis product of PMMA is MMA ($C_5H_8O_2$):



The pyrolyzed reaction rate is

$$r = \left(\frac{\rho_s}{\rho_{s0}} \right) A_{solid} \exp\left(-\frac{E_{solid}}{RT_s} \right)$$

The gas-phase combustion reaction is approximated by a one-step second-order irreversible Arrhenius reaction. The combustion of monomer vapors with air can be written in term of the global reaction given by:



The thermophysical parameters and chemical reaction kinetics parameters of PMMA in the calculation are shown in Table 1. It is necessary to say that the ignition is a very complex problem, which is very sensitive as flammability limits are slowly crossed in the study. And thus, the kinetic parameters were carefully selected. Staggs (1999, 2014) compared thermal degradation of polymers using single-step equation with the n th-order Arrhenius equation, and confirmed that the equivalent first-order approximation applied to a global in-depth model of PMMA degradation can provide a sufficiently good agreement with experimental results. Previous simulation works, which were paid attention on piloted ignition, preferred first-order Arrhenius

Table 1 Physical properties of the PMMA, as well as solid and gas phase kinetic parameters

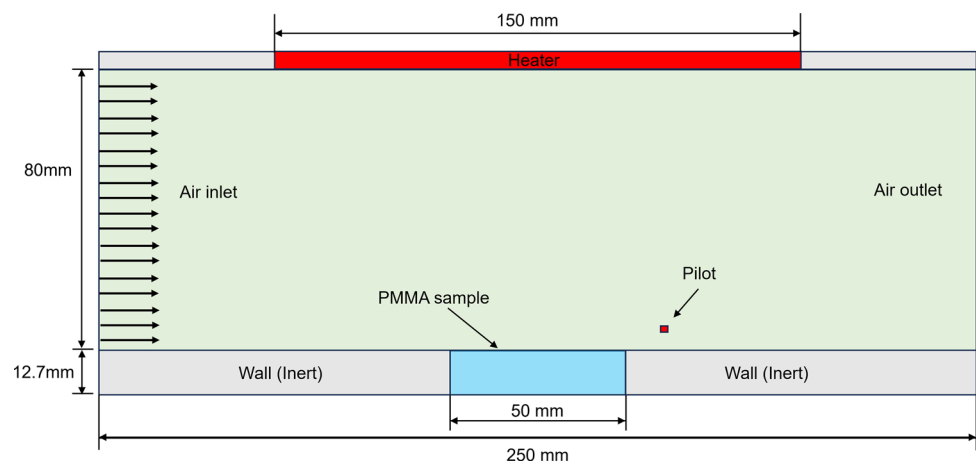
	Parameter	Symbol	Units	Value
PMMA thermophysical property parameters	Density	ρ	kg/m ³	1190
	Specific Heat	C_p	J/kg/k	1100
	Conductivity	k	W/m k	0.13
	Emissivity	ϵ		0.9
	Absorption Coefficient	C	1/m	800
Solid Phase	Heat of Reaction	$\Delta H_{s \rightarrow g}$	kJ/kg	1100
	Activation Energy	E_{solid}	kJ/mol	125
	Pre-Exponential Factor	A_{solid}	1/s	2.8E9
Gas Phase	Activation Energy	E_{gas}	kJ/mol	189
	Pre-Exponential Factor	A_{gas}	cm ³ /mol/s	1.0E16
	Heat of Combustion	ΔH_{comb}	MJ/kg	25.2

kinetics to model the oxidative and thermal pyrolysis of the matrix for the ignition (Lautenberger et al. 2005; Zhou et al. 2000, 2002, 2003; Fereres et al. 2012) and combustion (Kacem et al. 2016; Rakesh Ranga et al. 2018) of a PMMA plate. Following the abovementioned works, we select the parameters which were used in this work. The DNS mode in FDS has successfully been used in the past for similar piloted ignition models of composite materials (Fereres et al. 2012; Lautenberger et al. 2005). There are also other examples where FDS in DNS form has been used to model flame spread and has been compared to experimental results, all of which are suggested as verification for this use of FDS (Mcdermott 2022).

The computational domain is shown in Fig. 1. In the streamwise x -direction, it is 250 mm long, and in the cross-stream z -direction, it is 92.7 mm high. The inlet boundary condition on the $-x$ of the domain induces a prescribed velocity, which assumes that the oxidizer enters into the tunnel evenly from the inlet. The $+x$ domain is kept as an “open” boundary condition. A certain temperature radiant heating panel with a length of 150 mm, which generates radiant heat flux by setting the surface

temperature, is embedded in the middle part of the upper wall ($z = 92.7$ mm). The upper wall of the upper tunnel floor is set as inert properties. The fuel sample with a size of 50 mm long and 12.7 mm thick is embedded in the bottom tunnel floor. The sample holder is simply modeled as an insulated surface at the unexposed side of the fuel sample. The pilot igniter, which is sized as a single grid, located 10 mm downstream from the sample and 3.5 mm above the tunnel floor. The surface temperature of the pilot igniter is kept at a constant of 1623 °C to minimize the gas-phase induction time. To minimize the effect of the radiation on the trailing edge of the sample, the emissivity of the igniter is kept at 0.01. The mesh division is based on Fereres et al. (2012, 2015), and to make the results more accurate, a finer mesh is used in this paper, and the mesh size used for the whole area is 1 mm in the x -direction and 0.5 mm–0.6 mm in the z -direction. The separate grid sensitivity analysis is performed, and shown in the Appendix.

For incoming flow, the mass fraction of oxygen and nitrogen are set as 0.23 and 0.77, respectively. The initial temperature is 20 °C. The microgravity level is 10^{-6} g. The airflow velocities are in a range of 40 cm/s to 3 cm/s. The

Fig. 1 Computational domain configuration

time step used in the model is an adaptive time step, which is about 0.07–0.08 s.

The PMMA thermophysical property parameters as well as the chemical reaction kinetics parameters, which are shown in Table 1, were adjusted through a pilot ignition test in the experimental apparatus using the PMMA samples which are used in our previous microgravity works (Zhu et al. 2019). Parameters from Fereres et al. (2012) in a high-velocity flow environment were also used to calculate for comparison, and results showed that the ignition behaviors, variation of ignition delay time and the critical parameters with airflow velocity agree qualitatively with each other. Only the results using the parameters in Table 1 were shown and analyzed in this paper.

Results and Discussion

The Ignition Process

Piloted ignition of a thermally irradiated combustible solid begins with the development of a thermal decomposition layer near the irradiated surface. Typical distributions of fuel/oxygen mass fraction with the external radiant heat flux of 16 kW/m² are shown in Fig. 2, showing how the premixed flame becomes diffusion flame except in the small upstream region, which is termed as flame front (see Videos S1 and S2). Under $V_g = 3$ cm/s, at $t = 63$ s, the volatile compounds released from the pyrolyzed solid fuel diffused and convected outward to mix with ambient air. After a period of pyrolysis, at $t = 86.8$ s, a premixed flame is formed at downstream of the fuel sample, and products are filled in this region. At $t = 89.53$ s, the reaction zone propagates upstream, and the fuel gas zone shrinks, corresponding to a flash behavior. After a period of flashing, a concurrent diffusion flame becomes anchored at the fuel surface when the generation rate of pyrolyzed vapors is sufficient to sustain the flame. In the fire field, it is identified as the “flash point” for the consistency with the flash, and “fire point” is identified for the establishment of fire points for liquid fuels. The fire point, or onset of sustained burning, is usually taken as the moment of ignition.

During the ignition process, the fuel pyrolyzate upstream of the solid material can mix with the incoming air to form a diffusion flame. With decreasing flow velocity, an inadequate oxidizer supply makes sustained combustion difficult, and the flame extinguishes instantly. Following this, the solid surface continues to be heated and the pyrolysis rate of the solid fuel continues to increase, the insufficient oxidizer is unable to support the combustion of the pyrolyzate. The result of the establishment of a stable diffusion flame indicates that an inner rich premixed zone is formed for the formation of a stable flame. Furthermore, a thicker

fuel boundary layer develops upstream of the solid at low velocity flow (Fig. 2a), which on the one hand allows the flame to reside at the front end of the solid with sufficient fuel pyrolyzate to support combustion at a lower concentration than that above the solid surface, and on the other hand, increases the contact area between the fuel and the oxygen as a means of establishing a stable diffusion flame under the conditions of lack of oxidant.

The mass fraction of fuel and oxygen during PMMA ignition process under microgravity conditions at an air-flow velocity of 40 cm/s is shown in Fig. 2b. It is seen that the fuel-air mixture is limited to a thin layer near the fuel surface. When the fuel/air mixture near the piloted is above the flammability limit, a flame will be formed. As the rate of pyrolyzate grows, the reaction rate region around the piloted increases. At $t = 136.72$ s, the reaction rate ‘jumps’ upstream onto the solid surface in the form of a premixed flame propagating through a premixed mixture, consuming most of the fuel except in a very narrow layer (quenching layer) near the solid surface. During this propagation process a kind of triple flame is generated. Finally, at $t = 140.08$ s, the premixed flame propagates across the whole solid surface and a diffusion flame is established over the solid surface.

The flash flame is also found in the normal gravity environment in ambient pressure and low-pressure environments (Fereres et al. 2012, 2011; Rich et al. 2007). Figure 3 shows the time evolution of the fuel and oxygen mole fraction around the pilot under different air flow velocities. The time between the premixed time which is jumping on the solid surface (flashing condition) and a diffusion flame which is anchoring on the surface (sustained burning) decreases with the flow velocity.

Ignition Delay Time

Numerical flash time, ignition delay time and the duration of the flashing as a function of airflow velocity with radiative heat flux of 16 and 25 kW/m², together with previously reported microgravity experimental data from NASA KC-135 aircraft (Roslon et al. 2000) under 25 kW/m² and 35 kW/m² are presented in Fig. 4. The numerical results showed that, the time for the first flash and the flash duration time have opposite trends with the change in airflow velocity: the time of the first flash decreases with decreasing the flow velocity, whereas that of the flash duration increases monotonically with the decrease in V_g , and moreover, the rate of increase accelerates drastically as V_g approaches the flammable limit. As a consequence, the ignition delay time, which is defined as the time for a formation of a sustained flame undergoes a rapid growth with the approach of a limited flow velocity, until no ignition was occurred at a certain quenching limit. The variation trend of the ignition delay time with reduced

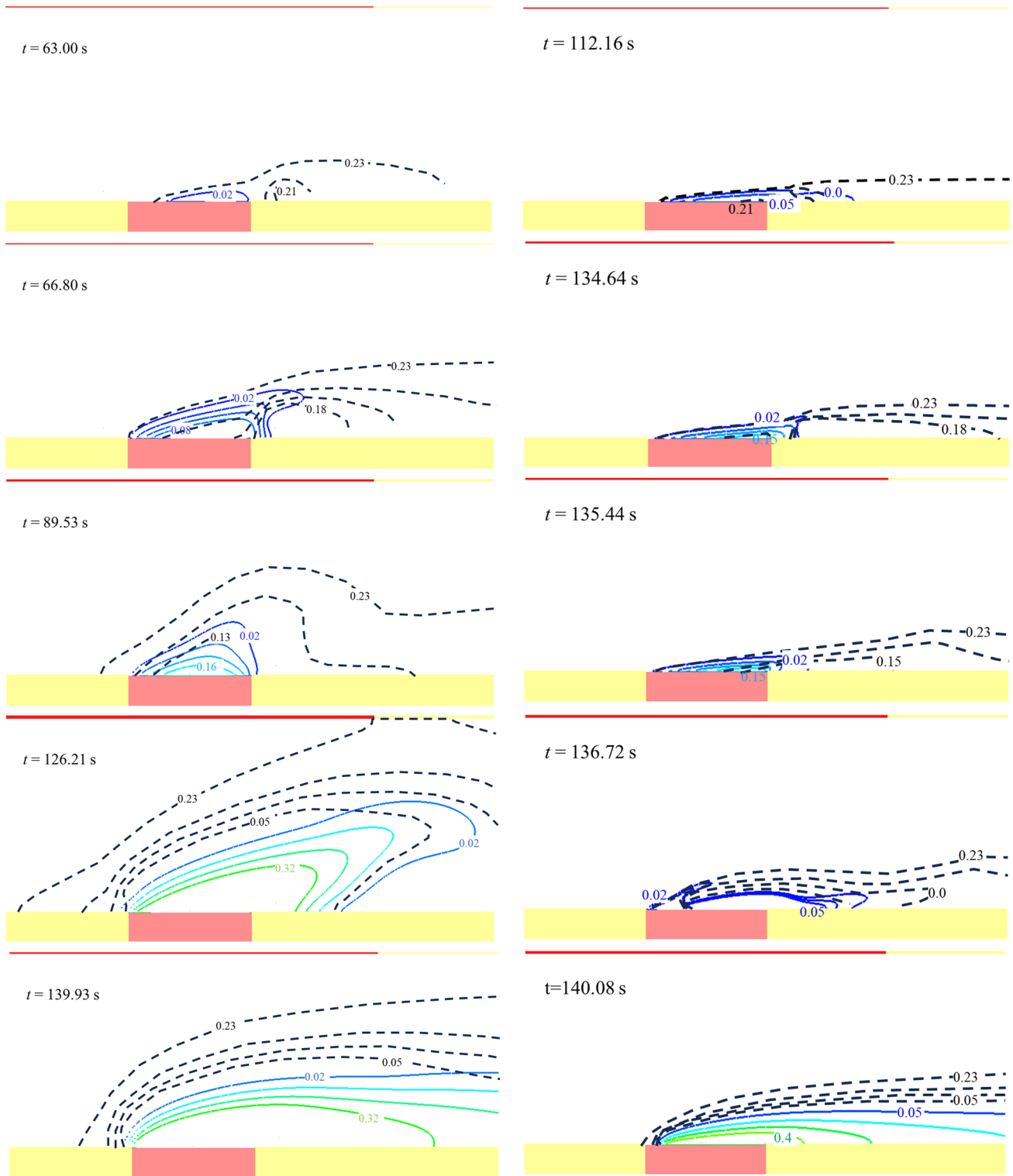
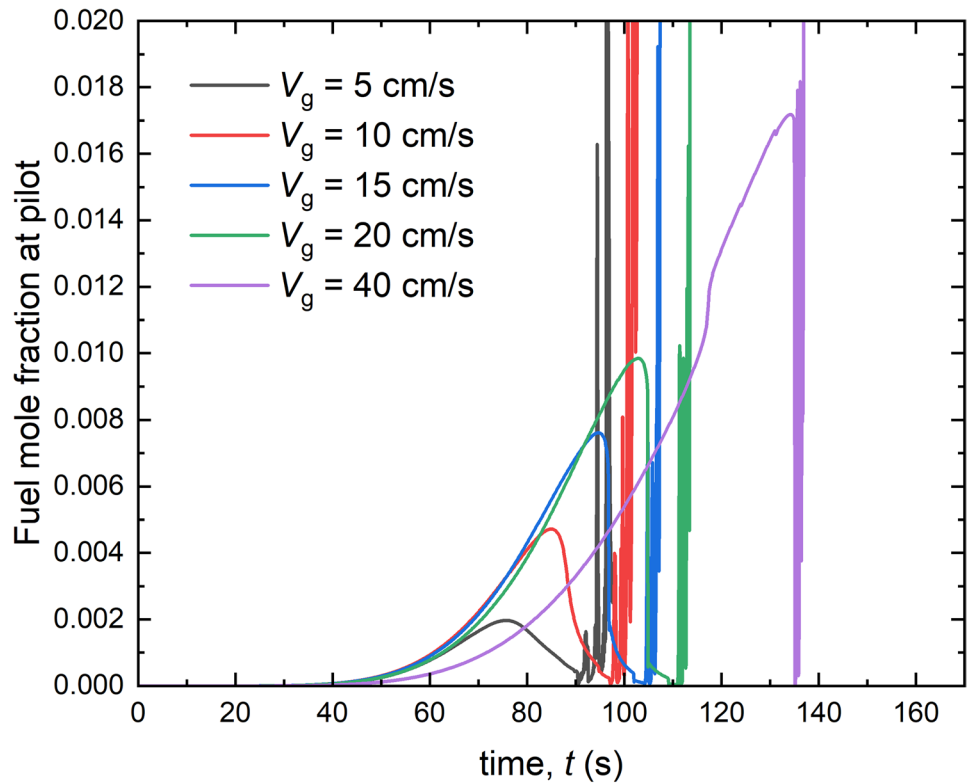


Fig. 2 Fuel and oxygen mass fraction contours for **a** $V_g = 3$ cm/s (left) and **b** $V_g = 40$ cm/s (right) with a radiative heat flux of 16 kW/m^2 . The dash lines and solid lines correspond, respectively, to the oxygen mass fraction and fuel mass fraction

flow velocity is in contrast to that from the previous microgravity experiments, which decreases with the reduced velocity monotonously. It should be noted that as Roslon et al. (2000) pointed out the g-jitter, which refers to small fluctuations in the g-level due to the meteorological

and physical events, is one of the difficulties. Buoyant flows induced by such fluctuations may exceed the very low forced flow velocities (below ~ 0.09 m/s) and result in increased ignition delay. The simulations in this paper show that the flash duration is very sensitive to

Fig. 3 Variation of fuel and oxygen mole fraction with time at the igniter location ($\dot{q}_e'' = 16 \text{ kW/m}^2$)



the external flow velocities, and that very low-velocity airflow may have a large impact on the experiments. It implies that the ignition of thermally thick solid fuel with low-velocity airflow deserves more experimental research. In the low-velocity air flow environment, with the increase of the radiative heat flux, the time for the

first flash, the flash duration time and the ignition delay time decreases. The variation trend of ignition delay time with the radiative heat flux is in accordance with that in the high-velocity flow environment (Cordova et al. 2001; Zhou and Fernandez-Pello 2000; Zhou et al. 2003), though the flame only flashes few times with high flow velocity.

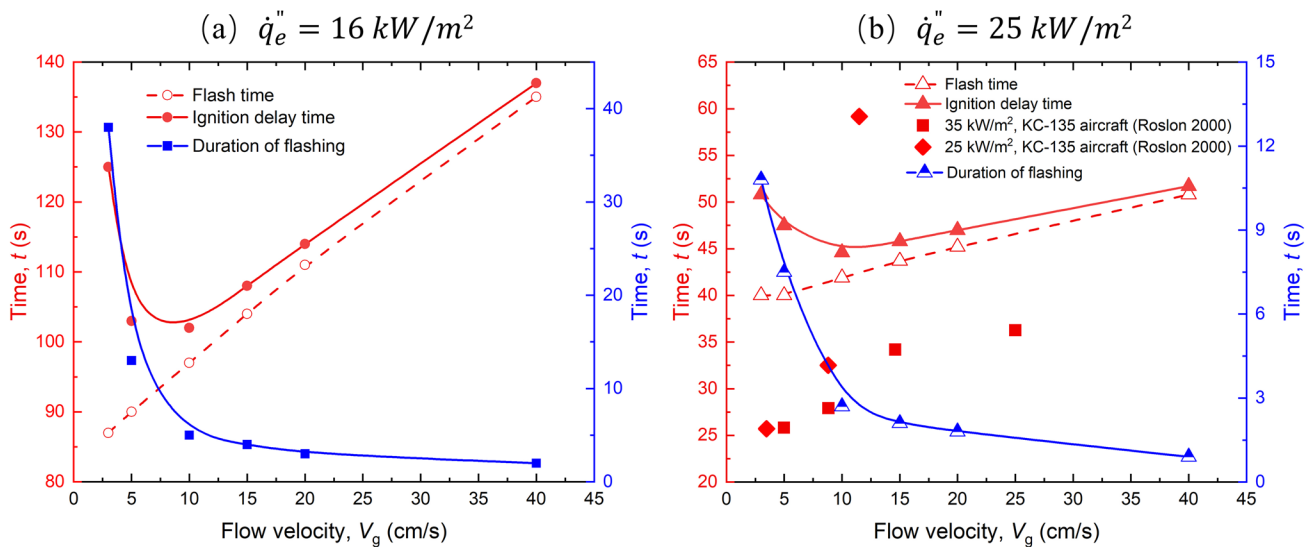


Fig. 4 The first time for flame flash (flash time), ignition delay time and the duration of flame flashing as a function of flow velocity under a $\dot{q}_e'' = 16 \text{ kW/m}^2$ and b $\dot{q}_e'' = 25 \text{ kW/m}^2$ in air conditions

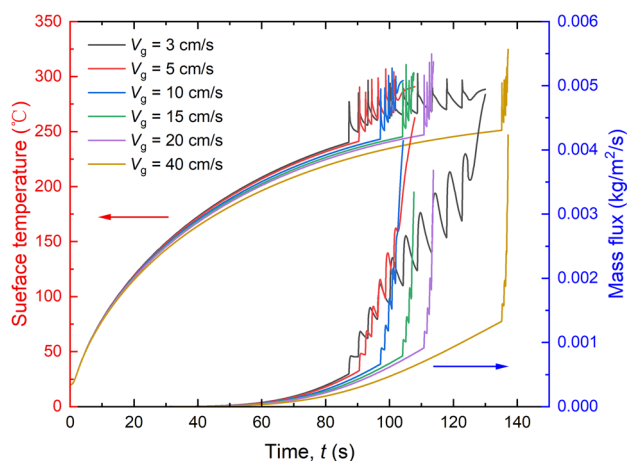


Fig. 5 The evolution of the solid surface temperature and mass flux at $\dot{q}_e'' = 16 \text{ kW/m}^2$

Ignition Critical Parameters

Figure 5 shows the time evolution of the solid surface temperature and mass flux at $\dot{q}_e'' = 16 \text{ kW/m}^2$. It is clear that at the time when the flame flashing first occurs, the surface temperature and mass flux were significantly increases. In the environment with a high airflow velocity, the temperature increases rapidly when the fire flashing occurs with a large frequency in a short time. While the airflow velocity is lower, flame flashes with a small frequency for a long time. At the time when a sustained flame was anchored on the fuel surface, the surface temperature and mass flux increased with a steep slope, which may pose a relative error for the results. The surface temperature and mass flux at first flame flash and ignition as a function of flow velocity

have been shown in Fig. 6. Results showed that the surface temperature at ignition increases with increasing the airflow velocity, which agrees with the experimental observations (Cordova et al. 2001; Zhou et al. 2002, 2001). However, the critical mass flux at ignition decreases with increased the flow velocity and then increases. When the airflow velocity is higher than 10 cm/s, the variation of the critical mass flux at the fire point is in accordance with previous studies (Rich et al. 2007; Zhou et al. 2001, 2002).

To gain insight into the mechanisms underlying the different variation trend of critical flux and critical surface temperature, we proceed to carry out a heat transfer analysis at the fuel sample surface. Figure 7 shows the time history of net heat flux at the middle of the fuel sample surface under different airflow velocities. Before the fuel is ignited, the net heat flux increases at the solid surface increases with the reduced airflow velocity. However, at the ignition time, the net heat flux increases with the increased airflow velocity, making a larger surface temperature, as is shown in Fig. 8. By contrast, the internal temperature is affected by both the external heat flux and the surface temperature, which provide more heat flux to the solid. It is clear that at $V_g = 3 \text{ cm/s}$ and 40 cm/s , the internal temperature near the fuel surface is relatively high, corresponding to a longer applied time and a larger surface temperature respectively. The higher temperature promotes the pyrolysis of the internal solid fuel, resulting of an increase in the fuel mass flux at ignition.

Discussion

Previous correlation studies have attributed the presence of flash to fuel generation rates that are insufficient to sustain a flame (Roslon et al. 2000), but the fact may be more

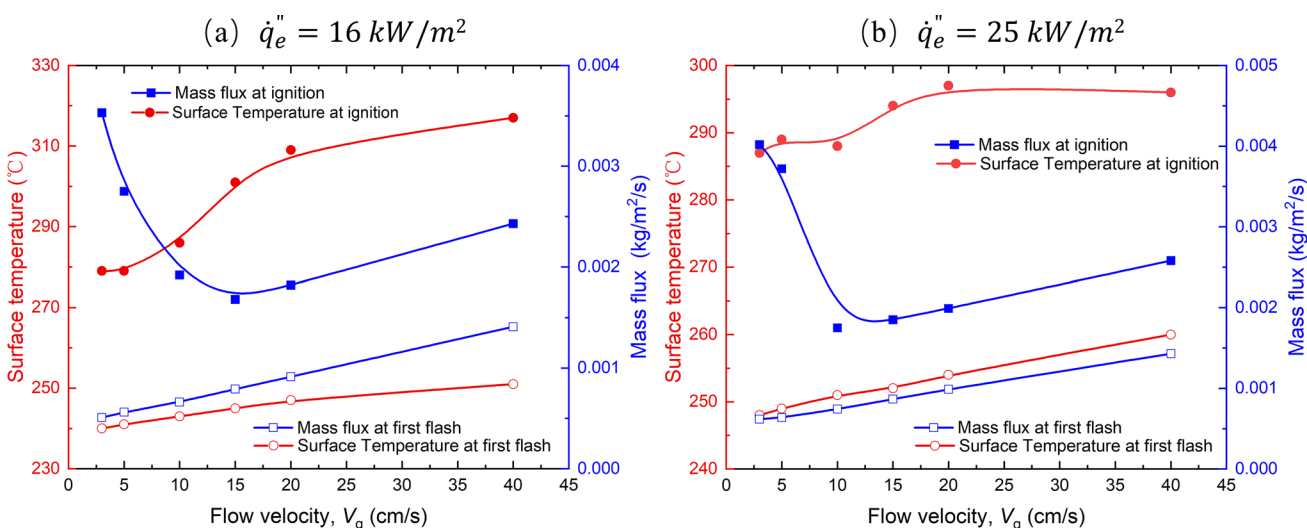


Fig. 6 The surface temperature and mass flux at first flame flash (flash time) and ignition as a function of flow velocity under **a** $\dot{q}_e'' = 16 \text{ kW/m}^2$ and **b** $\dot{q}_e'' = 25 \text{ kW/m}^2$

Fig. 7 Time history of net heat flux at the middle of the fuel sample surface under different airflow velocities under $\dot{q}_e'' = 16 \text{ kW/m}^2$

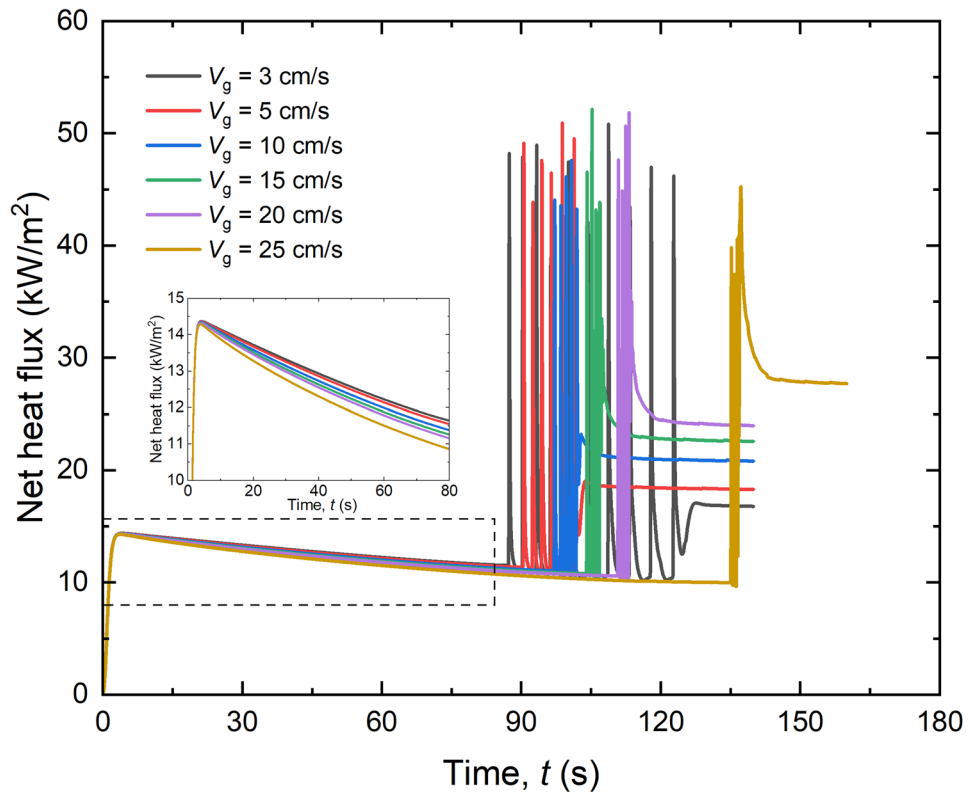


Fig. 8 Solid phase temperature distribution at the middle of the sample with different airflow velocities at the ignition time under $\dot{q}_e'' = 16 \text{ kW/m}^2$

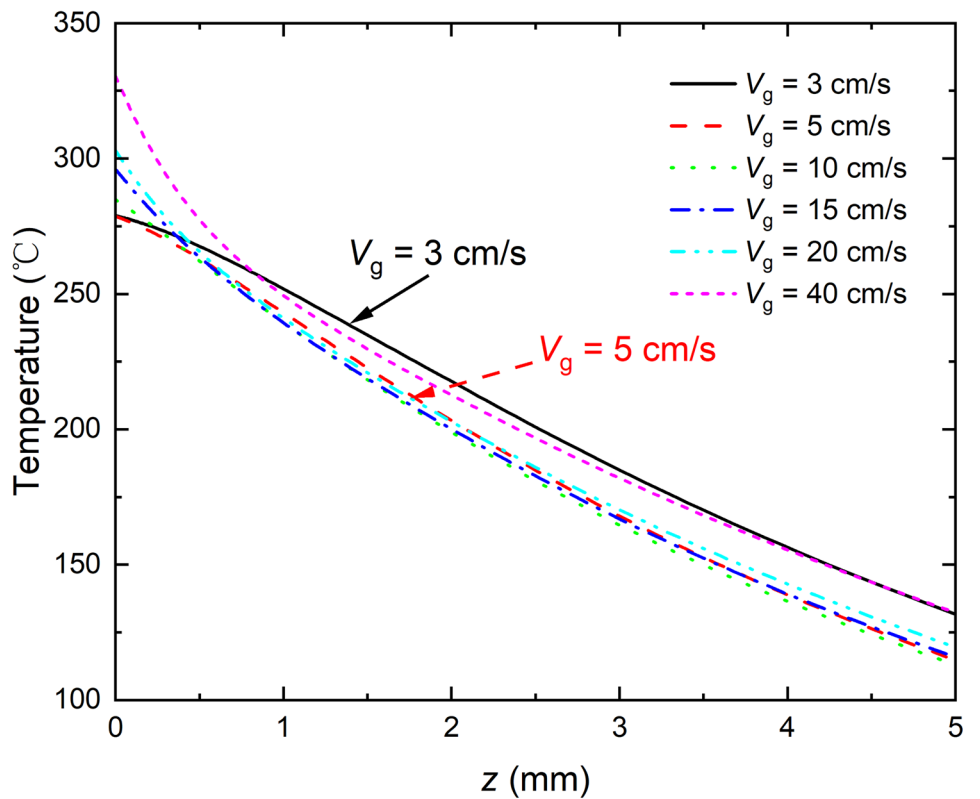
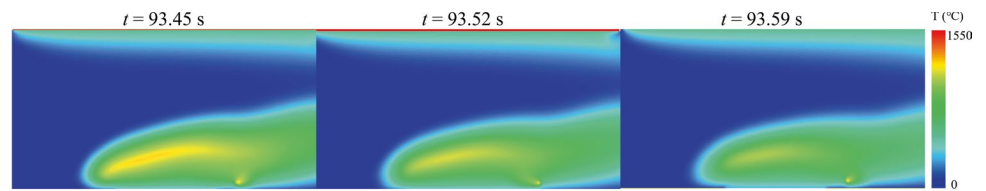
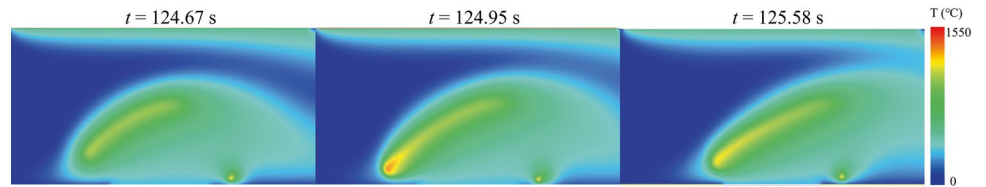


Fig. 9 Gas phase temperature before ignition $\dot{q}_e'' = 16kW/m^2, V_g = 3\text{ cm/s}$



(a) temperature distribution after flash



(b) temperature variation after the last flash

complex. If flame flash in high-velocity flow is considered as a component of the ignition even, the flash in low-velocity flow environments is more likely to be independent of the ignition event. From a mass distribution point of view, the fuel boundary layer continues to expand during a sustained flash to the point where the flame is more like floating in the air than attached to a solid. In terms of gas-phase temperature, an ignition kernel is produced first at the pilot and then the flame spreads, which has a high gas-phase temperature, but the temperature decreases rapidly and the flame dissipates, this process repeated during the flashes (Fig. 9a). However, in the last flash before ignition, the gas-phase

temperature started to descend like before, but then a high-temperature region reappeared at the upstream of the solid fuel region, and the flame can be sustained. (Fig. 9b).

Considering that both oxidant and fuel are required for flame maintenance, we investigated the oxidant distribution profile and the fuel distribution profile together (Fig. 10). It was noted that because of the thicker fuel boundary layer, the flame propagated in the region higher from the solid while consuming a large amount of oxygen and creating an oxygen hole around the solid material. The pyrolysis gases remaining above the solid cannot reach the oxidant and the combustion reaction is forced to abort. When the mixture of

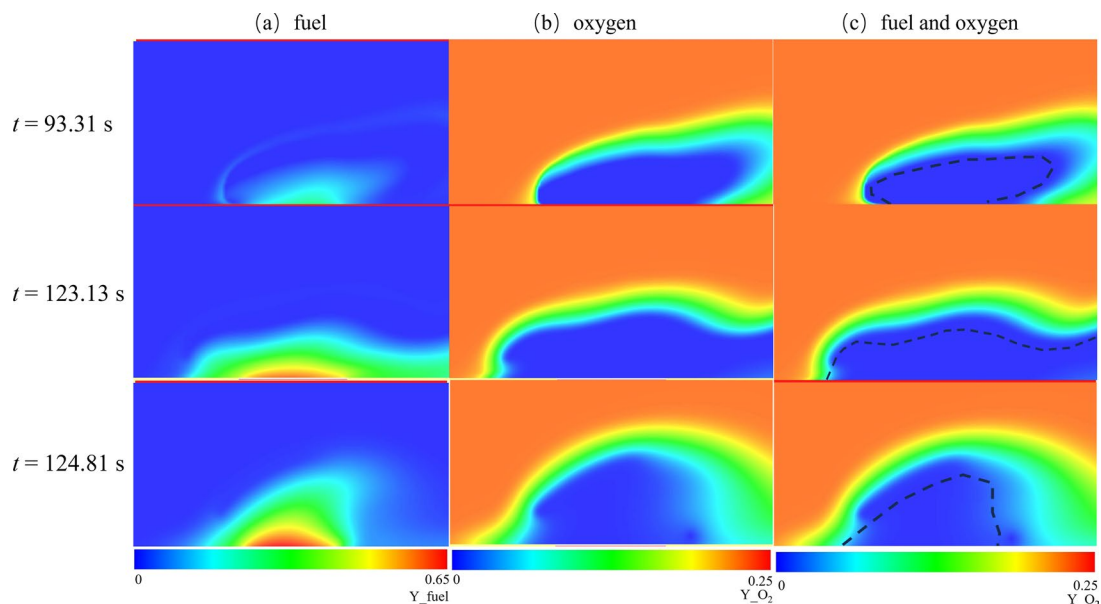
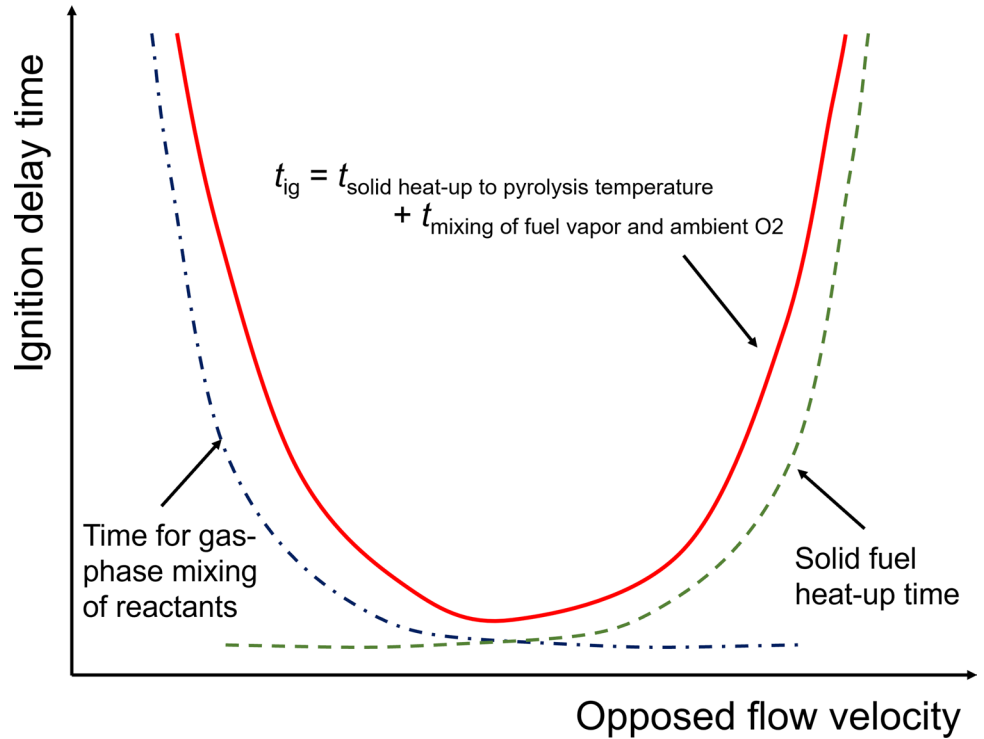


Fig. 10 Map of fuel (a), oxygen distribution (b) after flash at different times, and their overlapping form (c). The black dotted line donates the fuel boundary

Fig. 11 Ignition delay times with the controlling mechanisms identified



incoming stream of oxidant and the pyrolysis fill the hole, the flame flashes again. After several flashes, the rate of pyrolysis rate increases and the fuel has a higher diffusion rate. At the end of one of the flashes, the combustion reaction almost stops, followed by a rapid occupation of the oxygen hole by the residual high concentration of pyrolyzate, then the pyrolyzate overlaps the boundary with the oxidant, In the high temperature environment, the combustion reaction starts again. Because there is no flame flash consuming excessive amounts of oxygen during this combustion reaction, the flame eventually continues in a weak form.

Apparently, the flame flash behavior is mainly attributes to the lack of oxygen supply of the reaction region. When the ambient flow rate increases and the reaction region is able to consistently receive sufficient oxidant, a stable flame will be established without flame flashes. Preliminary study suggests that such the ambient flow velocity is about 10 cm/s in air conditions.

Ignition of solid materials is a coupled process of gas-phase and solid-phase reactions, and for the piloted ignition, the chemical time can be ignored (Quintiere 2006). As discussed in the former section, the mixing process

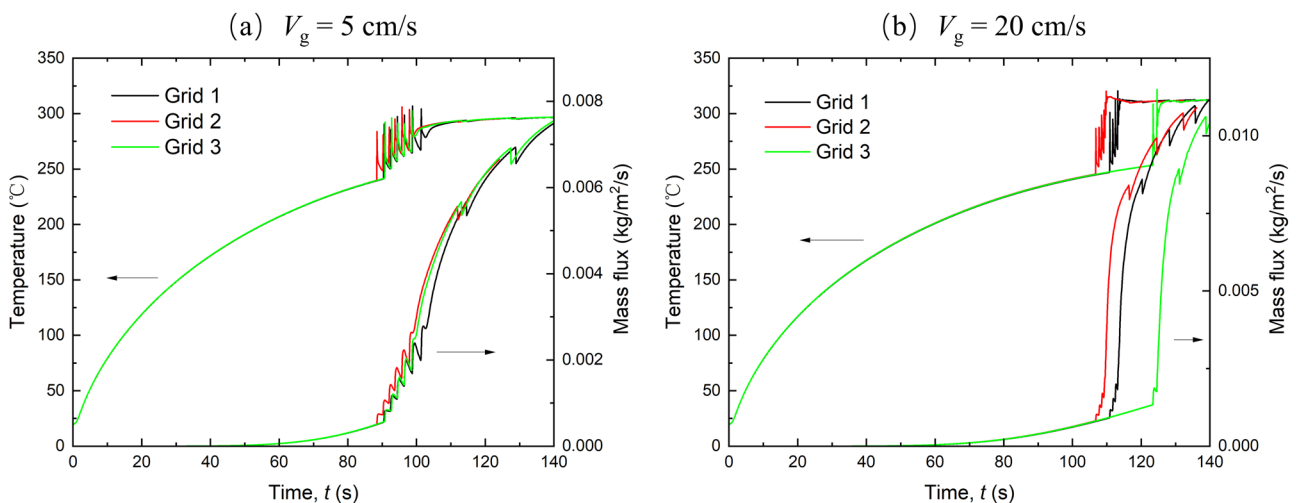


Fig. 12 Calculated results for different grids

plays an important role in the solid ignition in the low flow velocity environment, while in the high flow velocity conditions, the pyrolysis process dominates the solid ignition (Quintiere 2006). The controlling mechanisms identified for the ignition delay times is outlined in Fig. 11. With the increased opposed flow velocity, the time for gas-phase mixing of reactants decreases while the solid fuel heat-up time increases. Then there is a critical flow velocity for the appearance of a minimum ignition delay time. In the present study, an airflow-velocity of 5–10 cm/s was been identified. The gas-phase mixing/reaction dominates the ignition process of a thermally-thin solid fuel (Olson 2011), and results have shown that with a 100 kW/m^2 radiative heat flux, the ignition delay time increases at low -velocity flow (Fig. 11).

Conclusion

In this research, a two-dimensional numerical model was established using Fire Dynamics Simulator software to investigate the effects of airflow velocity on the ignition characteristics of a thermally-thick solid fuel with external radiative heat flux in the microgravity environment. Two radiant heat flux, which are 16 and 25 kW/m^2 were studied, and an external airflow was varied from 0 to 40 cm/s. The focus is to reveal the effects of gas-phase mixing/reaction on the variation of the ignition delay time of thermally thick solid fuel in the buoyant-free environment with low-velocity flow, and ignition behaviors were investigated in detail. The critical temperature and mass flux were summarized. The main results are as follows:

1. Two distinct ignition process were identified, namely the premixed flame formation process, characterized by flashing over a period of time, and a stable diffusion flame process, characterized by a sustained concurrent flame. The time of flash appears with the increase of air velocity shows an increasing trend and is consistent with the pyrolysis theoretical model. Flash duration decreases rapidly with increasing airflow velocity, the mechanism of which may be accounted for by the slow mixing of the pyrolyzate with the oxidizer in the external airflow.
2. The ignition time, which is defined as the time when a continuous flame is attached to the fuel surface, decreases, reaches a minimum, and then increases until ignition does not occur. Mechanisms were considered to explain the “V-shaped” dependence of ignition time on flow-velocity, and two regimes were identified each having a different controlling mechanism: the mass transport regime where the ignition delay is controlled

by the mixing of oxygen and pyrolysis; and the heat transfer regime where the ignition delay is controlled by changes in convection heat losses and critical mass flux for ignition.

3. With the decrease of the airflow velocity, the critical mass flux shows a trend of decreasing and then increasing, which is dominated by the mixing of the pyrolyzate and the oxidizer, while the critical temperature monotonically decreasing, which is dominated by a reduce of the net heat flux at the fuel surface.

Appendix

In this study, the grid independence test was carried out by using three different grid numbers 34400 (Grid1, 1 mm in the x -direction and 0.6 mm in the z -direction), 24,960 (Grid2, 1.3 mm in the x -direction and 0.8 mm in the z -direction), and 15560 (Grid3, 2 mm in the x -direction and 1.2 mm in the z -direction), the mesh near the solid surface was refined to $1 \text{ mm} \times 0.1 \text{ mm}$. The surface temperature and mass flux at the middle of the fuel with an airflow velocity of 5 cm/s and 20 cm/s were shown in Fig. 12. It can be seen that, at lower airflow velocity, the temperature and mass flux are almost the same for the three Grids. At higher flow velocities, there are some differences between the results for the coarsest and the finest meshes, but these differences decrease rapidly as the mesh is refined. In this work, the grid number 34400 (Grid 1) was adopted in the simulations considering both the accuracy and cost of the computation.

Supplementary Information The online version contains supplementary material available at <https://doi.org/10.1007/s12217-023-10092-7>.

Author Contributions KZ: Investigation, Methodology, Writing – original draft. FZ: Conceptualization, Supervision, Project administration, Writing – review & editing. SW: Investigation, Project administration, Writing – review & editing.

Funding National Key R&D Program of China under Grant No. 2021YFA0716203, Young Elite Scientists Sponsorship Program by BAST under Grant No. BYESS2023440, and the opening project of CAS Key Laboratory of Microgravity under the grant No. NML202301.

Availability of Data and Materials The data that support the findings of this study are available from the corresponding authors upon reasonable request.

Declarations

Ethical Approval This research does not include any material that require ethical approval.

Conflict of Interest The authors declare no competing interests.

References

- Cordova, J.L., Walther, D.C., Torero, J.L., Fernandez-Pello, A.C.: Oxidizer flow effects on the flammability of solid combustibles. *Combust. Sci. Technol.* **164**, 253–278 (2001). <https://doi.org/10.1080/00102200108952172>
- Fereres, S., Fernandez-Pello, C., Urban, D.L., Ruff, G.A.: Identifying the roles of reduced gravity and pressure on the piloted ignition of solid combustibles. *Combust. Flame* **162**, 1136–1143 (2015). <https://doi.org/10.1016/j.combustflame.2014.10.004>
- Fereres, S., Lautenberger, C., Fernandez-Pello, A.C., Urban, D.L., Ruff, G.A.: Understanding ambient pressure effects on piloted ignition through numerical modeling. *Combust. Flame* **159**, 3544–3553 (2012). <https://doi.org/10.1016/j.combustflame.2012.08.006>
- Fereres, S., Lautenberger, C., Fernandez-Pello, C., Urban, D., Ruff, G.: Mass flux at ignition in reduced pressure environments. *Combust. Flame* **158**, 1301–1306 (2011). <https://doi.org/10.1016/j.combustflame.2010.11.013>
- Fernandez-pello, A.C.: The solid phase. In: *Combustion fundamentals of fire*. pp. 31–100 (1995)
- Fujita, O., Takahashi, J., Ito, K.: Experimental study on radiative ignition of a paper sheet in microgravity. *Proc. Combust. Inst.* **28**, 2761–2767 (2000). [https://doi.org/10.1016/S0082-0784\(00\)80697-9](https://doi.org/10.1016/S0082-0784(00)80697-9)
- Kacem, A., Mense, M., Pizzo, Y., Boyer, G., Suard, S., Boulet, P., Parent, G., Porterie, B.: A fully coupled fluid/solid model for open air combustion of horizontally-oriented PMMA samples. *Combust. Flame* **170**, 135–147 (2016)
- Lautenberger, C., Torero, J., Fernandez-Pello, C.: Understanding material flammability. *Flammabl. Test. Mater. Used Constr. Transp. Mining*, Second Ed. 1–22 (2021). <https://doi.org/10.1016/B978-0-08-102801-8.00066-1>
- Lautenberger, C.W., Zhou, Y.Y., Fernandez-Pello, A.C.: Numerical modeling of convective effects on piloted ignition of composite materials. *Combust. Sci. Technol.* **177**, 1231–1252 (2005). <https://doi.org/10.1080/00102200590927058>
- McAllister, S., Fernandez-Pello, C., Urban, D., Ruff, G.: The combined effect of pressure and oxygen concentration on piloted ignition of a solid combustible. *Combust. Flame* **157**, 1753–1759 (2010). <https://doi.org/10.1016/j.combustflame.2010.02.022>
- Mcdermott, R.: Sixth edition fire dynamics simulator technical reference guide volume 1: Mathematical model. p. 1 (2022)
- McGrattan, K.B., Baum, H.R., Rehm, R.G., Hamins, A., Forney, G.P., Floyd, J.E., Hostikka, S.: Fire dynamics simulator (version 3)-Technical reference guide. National Institute of Standards and Technology, NISTIR 6783 (2003a)
- McGrattan, K.B., Forney, G.P., Floyd, J.E., Hostikka, S., Prasad, K.: Fire dynamics simulator (version 3)-User's guide. National Institute of Standards and Technology, NISTIR 6784 (2003b)
- Olson, S.L.: Piloted ignition delay times of opposed and concurrent flame spread over a thermally-thin fuel in a forced convective microgravity environment. *Proc. Combust. Inst.* **33**, 2633–2639 (2011). <https://doi.org/10.1016/j.proci.2010.06.020>
- Quintiere, J.G.: *Fundamentals of fire phenomena*. John Wiley & Sons (2006)
- Rakesh Ranga, H.R., Korobeinichev, O.P., Harish, A., Raghavan, V., Kumar, A., Gerasimov, I.E., Gonchikzhapov, M.B., Tereshchenko, A.G., Trubachev, S.A., Shmakov, A.G.: Investigation of the structure and spread rate of flames over PMMA slabs. *Appl. Therm. Eng.* **130**, 477–491 (2018)
- Rich, D., Lautenberger, C., Torero, J.L., Quintiere, J.G., Fernandez-Pello, C.: Mass flux of combustible solids at piloted ignition. *Proc. Combust. Inst.* **31**(2), 2653–2660 (2007). <https://doi.org/10.1016/j.proci.2006.08.055>
- Roslon, M., Olenick, S., Walther, D., Torero, J.L.: Microgravity ignition delay of solid fuels in low velocity flows. *AIAA*. **39**(12), 2336–2342 (2000). <https://doi.org/10.2514/6.2000-580>
- Staggs, J.E.J.: Modelling thermal degradation of polymers using single-step first-order kinetics. *Fire Saf. J.* **32**, 17–34 (1999)
- Staggs, J.E.J.: The effects of gas-phase and in-depth radiation absorption on ignition and steady burning rate of PMMA. *Combust. Flame* **161**, 3229–3236 (2014)
- Zhou, Y., Fernandez-Pello, A.C.: Numerical modeling of endothermic pyrolysis and ignition delay of composite materials exposed to an external radiant heat flux. *Proc. Combust. Inst.* **28**, 2769–2775 (2000). [https://doi.org/10.1016/S0082-0784\(00\)80698-0](https://doi.org/10.1016/S0082-0784(00)80698-0)
- Zhou, Y.Y., Walther, D.C., Fernandez-Pello, A.C.: Numerical analysis of piloted ignition of polymeric materials. *Combust. Flame* **131**, 147–158 (2002). [https://doi.org/10.1016/S0010-2180\(02\)00396-6](https://doi.org/10.1016/S0010-2180(02)00396-6)
- Zhou, Y.Y., Walther, D.C., Fernandez-Pello, A.C., Torero, J.L., Ross, H.D.: Theoretical prediction of microgravity ignition delay of polymeric fuels in low velocity flows. 39th Aerosp. Sci. Meet. Exhib. 44–50 (2001). <https://doi.org/10.2514/6.2001-471>
- Zhou, Y.Y., Walther, D.C., Fernandez-Pello, A.C., Torero, J.L., Ross, H.D.: Theoretical prediction of piloted ignition of polymeric fuels in microgravity at low velocity flows. *Microgravity Sci. Technol.* **14**, 44–50 (2003). <https://doi.org/10.1007/BF02873335>
- Zhu, F., Lu, Z., Wang, S., Yin, Y.: Microgravity diffusion flame spread over a thick solid in step-changed low-velocity opposed flows. *Combust. Flame* **205**, 55–67 (2019). <https://doi.org/10.1016/j.combustflame.2019.03.040>

Publisher's Note Springer Nature remains neutral with regard to jurisdictional claims in published maps and institutional affiliations.

Springer Nature or its licensor (e.g. a society or other partner) holds exclusive rights to this article under a publishing agreement with the author(s) or other rightsholder(s); author self-archiving of the accepted manuscript version of this article is solely governed by the terms of such publishing agreement and applicable law.